NASA Technical Memorandum 87699

NASA-TM-87699 19860019220

Gating Characteristics of Photomultiplier Tubes for Lidar Applications

John D. W. Barrick

AUGUST 1986

NASA Technical Memorandum 87699

Gating Characteristics of Photomultiplier Tubes for Lidar Applications

John D. W. Barrick
Langley Research Center
Hampton, Virginia

National Aeronautics
and Space Administration
Scientific and Technical Information Branch
1986

CONTENTS

1. Introduction

The photomultiplier tube (PMT) is an extremely sensitive, fast, and versatile radiant energy detector (ref 1) These characteristics are essential in meeting detector requirements of lidar systems for remote measurements of backscattered light from gases and aerosols in the atmosphere (refs 2 and 3). As high-altitude measurement platforms—such as the U-2 aircraft, space shuttle, and space station—become available for lidar atmospheric research, requirements for high gain and signal linearity in lidar detectors become more stringent (ref 4) However, the same inherent high gain and fast response signal characteristics that make the PMT ideal for lidar applications also make it vulnerable to extraneous noise from relatively high-intensity light levels and transients induced by gate pulses used for switching photomultipliers "on" and "off" Photomultiplier tubes are subjected to incident light levels that can span a wide dynamic range and may exceed current limits of the tube A method to decrease PMT gain by altering the voltage applied to the focus grid or selected dynodes can minimize saturation effects and signal induced gain changes within the PMT and subsequent electronics This method of gating the PMT can also affect gain stability Thus, a characterization of PMT's for their performance properties is necessary for an accurate and confident interpretation of lidar data

A detector test facility (DTF) has been developed and applied to characterize detector systems, which include PMT's, voltage-divider networks (bases), and associated electronics The DTF has been used in support of the multipurpose airborne differential absorption lidar (DIAL) system developed at the Langley Research Center (LaRC) The objective of this paper is to report on the DTF and its use in detector characterization studies and to obtain a data base for selecting optimum PMT and base configurations for DIAL applications For these applications, detectors should produce anode output signals with the following characteristics good gain stability, signal rise times of less than 1 μs after the leading edge of a switching pulse, and "hold-off" (the ability to prevent secondary photon emission) sufficient to avoid signal response problems associated with unwanted high light levels during minimum gain conditions

A brief description of the DIAL system is included to give better insight into test conditions and the characteristics critical to radiant energy detectors The following sections present (1) a description of the DTF and data acquisition system used in detector-package evaluations, (2) description of detector packages tested, (3) discussion of tests performed, (4) measurement techniques employed; and (5) observed detector signal characteristics The discussion of test results also includes a brief description and explanation of operation principles of the voltage-divider networks and PMT's investigated

2. DIAL System and Technique

The LaRC airborne lidar system uses the DIAL (differential absorption lidar) technique for the remote measurement of gas profiles in the atmosphere Only a general overview is presented here since both the DIAL system and measurement technique have been widely discussed (refs 2, 3, and 5) The DIAL technique determines the average gas concentration over some selected range interval by analyzing the differences between two backscattered laser signals which are tuned on and off a molecular absorption line of the gas under investigation The value of the average gas concentration $N(R_1, R_2)$ between two range points R_1 and R_2 can be determined from the ratio of the lidar signals and is given by

$$N(R_1, R_2) = \frac{1}{2(R_2 - R_1)(\sigma_{on} - \sigma_{off})} \ln \left[\frac{P_{off}(R_2)\, P_{on}(R_1)}{P_{off}(R_1)\, P_{on}(R_2)} \right]$$

In this relationship, $\sigma_{on} - \sigma_{off}$ is the difference between the absorption cross sections at the on and off wavelengths, and $P_{on}(R)$ and $P_{off}(R)$ are the lidar signals received from range R at the on and off wavelengths, respectively This analysis assumes that atmospheric backscattering parameters are equal at both wavelengths If there is an interfering gas which has a different absorption coefficient at these wavelengths, its concentration must be determined by an independent method The airborne DIAL system uses two frequency-doubled Nd YAG lasers to optically pump two tunable dye lasers which emit the desired on and off laser wavelengths These outputs are time separated to minimize receiver hardware requirements The time separation (approximately 100 μs) is a function of maximum aircraft altitude and is minimized to avoid DIAL concentration errors resulting from changes in atmospheric structure The dye laser output beams are directed out of the aircraft through a quartz window and are aligned coaxially with the receiver telescope The backscattered laser signals are then collected by the receiving telescope and directed onto the gated photomultiplier detectors Narrow band-pass interference filters are used to reject background light and any simultaneous returns at undesired wavelengths Each photomultiplier tube (PMT) is selected for optimum gain at the wavelength of interest, maximum linearity, and for minimal distortion related to electronic-tube gating

3. Detector Test Facility (DTF) Description

3.1. PMT Test Setup

Photomultiplier (PMT) evaluation and performance tests are accomplished by exposing PMT's to a pulsed light emitting diode (LED) mounted in a lighttight enclosure Both the PMT and base are attached to the enclosure in a manual-shuttered housing directly across from the LED The manual shutter protects the PMT from high light levels during test setup modifications The LED can be operated in various timing sequences with a variety of signal shapes LED current is varied by altering input voltage and in-line resistance PMT anode signals are held to approximately 400 mV or less through 50 ohms impedance to ensure that tube current limits are not exceeded

Precise timing signals are required to coordinate LED pulses with PMT gating sequences Overall timing and control signals of the DTF are supplied by the master control unit (MCU) Eleven gate pulses with 100-μs separation are provided at a 1-, 5-, or 10-Hz repetition rate by the MCU to a pulse generator which produces the desired PMT gating sequence pattern The pulse generator output signals are then amplified by a focus-gate driver board to voltage levels ($\leq$ 300 V) sufficient for gating a PMT by using the focus electrode or a dynode A PMT gate signal generator is optional and can be substituted for the pulse generator for added flexibility in gate sequence patterns Note that the purpose of multiple gate signals is to allow operational flexibility in selecting the on- and off-line signals in DIAL calculations Control signals are provided by the MCU to a Biomation 8100 Transient Digitizer for synchronization of data acquisition with LED pulses and PMT gating sequences A block diagram of the present test system configuration is shown in figure 1 A functional timing diagram for the master control unit is shown in figure 2

3.2. Data Acquisition System

The data acquisition system offers several modes of operation for processing and displaying the PMT analog signal output An oscilloscope is used to observe PMT signal levels to approximately 5 percent External video amplifiers are used to increase scope sensitivity, and video filters (5 0, 2 0, 1 0, 0 5, and 0 1 MHz) are available for the removal of high-frequency noise in PMT anode signals Further data processing capability is made possible by a Digital Equipment Corporation (DEC) PDP-11/10 minicomputer with 28K words of 16-bit RAM memory The PMT analog signal is digitized by a Biomation 8100 Transient Digitizer (8 bit) at an event sampling rate of 5 or 10 Hz Each event provides 2048 sequential samples at a rate of 10 MHz The digitized result is held in buffer memory and subsequently passed to the PDP-11/10 for processing and storage by means of a 16-bit parallel interface (DR11-C)

Processing capabilities available in the present software package for plotting PMT output signals individually or cumulatively include the following options signal averaging, background subtraction, variable X-Y scales, and signal offset subtraction DIAL concentration calculations can also be plotted to simulate the effects of a range-dependent gas absorption coefficient on the DIAL measurement Signal measurement accuracy of $\leq$ 1 percent can be obtained by using these data processing capabilities Only a brief description of the data processing system and capabilities was presented since a detailed discussion is included in the literature (ref 3)

4. Detector Description

4.1. Photomultiplier Tubes (PMT)

The photomultiplier tubes that were evaluated are listed in table 1 All the tubes tested were in-line dynode structured Data on the various PMT's are summarized from literature and technical data supplied by the tube manufacturers There are basically two categories of PMT's commonly used in lidar applications those with multialkaline photocathodes and those with bialkaline photocathodes Both tube types exhibit low noise characteristics and high quantum efficiencies in wavelength regions (290, 600, and 720 nm) desired in lidar applications The multialkaline photocathode tubes typically exhibit a higher quantum efficiency in the visible portion of the spectrum, while the bialkaline tubes perform more efficiently in the ultraviolet (UV) wavelength region Performance evaluations for these tubes were conducted with particular attention to variable gain characteristics seen in bialkaline cathode tubes used for UV detection in DIAL applications

4.2. Voltage-Divider Networks

Voltage-divider networks (bases) play a significant role in determining the performance characteristics of PMT's Presently, focus-grid-gated and dynode-gated bases are available for use with the DIAL system Focus-grid-gated bases include the voltage-divider networks (bases) designated "2," "4," and "6 " A circuit diagram of these bases is shown in figure 3 These circuits provide a positive high voltage pulse ($\approx$ 200 to 300 V) to the focus grid located between the cathode and dynode 1. This positive pulse allows photoelectrons to be focused

on dynode 1 for amplification An RCA AJ2132 adapter plug is used to accommodate 12-stage tubes in bases 2 and 4

In two additional bases, designated "A1" and "L-100-G," an alternative method using dynodes as the gating element is employed This method is similar to focus-grid gating with the exception that upper-stage dynode-emitted electrons are blocked by a negative dynode potential during the gate-off condition A dynode near the middle of the string should be used for this purpose (ref 1) Both the L-100-G and A1 bases use dynode 4, as shown in figures 4 and 5, respectively The dynode-gated bases are designed for 12-stage tubes and have not been adapted to the 14-stage tubes

Measured voltage distributions of available bases and the PMT manufacturers-recommended distributions are listed in table 2 with appropriate distribution codes for each type PMT listed in table 1

5. Measurements

5.1. Definitions

Photomultiplier characteristics that have a major impact on lidar detector operations include gain stability, hold-off, and rise time Reference to gain stability in this report refers to the ability of PMT output signals to exhibit minimum gain change during time periods of maximum gain conditions (< 200 μs) typical to lidar applications Hold-off, sometimes referred to as the "switching ratio," is defined to be the ability of a PMT to block relatively high-intensity light levels when gated "off" in order to avoid possible nonlinear signal effects following such events Rise time is defined as the time difference between 10- and 90-percent amplitude points of the leading edge of an anode signal after being gated on The development of the PMT test facility makes it possible to determine these characteristics quantitatively A rectangular LED pulse is predominantly used because gain-change, hold-off, and rise-time measurements are easily interpreted The tests performed to make the quantitative measurements necessary for performance evaluations are described in section 5 2 A discussion of tube characteristics and performance is discussed in section 6

5.2. Test Method

Hold-off and rise-time measurements for a wide selection of PMT's and bases have been made by exposing the selected detector package combination to a wider light pulse in time than the signal used to gate the PMT "on " By using sequence control signals from the master control unit to a pulse generator, a 40-μs-wide gate signal was produced every 100 μs for 11 pulses at a repetition rate of 1, 5, or 10 Hz This timing sequence is illustrated in figure 6(a) The master control unit also provides, in synchronization with the gate signal, a continuous 10-kHz clock pulse to a pulse generator which then supplies 80-μs-wide pulses to the LED as shown in figure 6(b) Red and green LED's, with wavelengths of approximately 640 and 488 nm, respectively, are interchangeable and selected with reference to the spectral response characteristics of the PMT being tested A green LED was used with the bialkaline cathode tubes and a red LED with the multialkaline tubes The 10-kHz clock is used to pulse the LED continuously to ensure equilibrium of the LED radiation output as seen by the PMT

Examples of an anode signal during a tube-gating sequence and an individual gate pulse are shown in figures 7(a) and (c), respectively The focus-gate signal is shown in figure 7(b) Initial observations of gain stability characteristics are made from frames of this type More precise signal measurements require the anode signal to be digitized and averaged by the data acquisition system Figure 8 depicts a digitized 200-shot average of an inverted anode signal during a single 40-μs-wide gate pulse A listing of each digitized point up to a 0 1-μs sampling rate and averaged over 1 to 200 shots, each with 8-bit accuracy, was used for determining the degree of gain stability during gate pulses

Hold-off measurements were made by comparing a 200- to 400-mV anode signal produced when illuminated by the LED during the gate-on period to the area of the anode signal with the gate off An example of the anode signal used for comparison is shown in figure 9(a) The gate-on condition, represented by the 200- to 400-mV portion of the anode signal, is bordered by a substantially lower signal representing the gate-off condition In figure 9(b), the tube was gated off and the oscilloscope sensitivity increased to 2 mV/cm This allowed the output signal with the tube in the off condition, sometimes referred to as "bleedthrough," to be more accurately measured

The rise-time measurement, as defined, is accomplished by increasing the oscilloscope sweep speed to 1 μs/cm to expand the leading edge of the anode signal as the tube is gated on as shown in figure 10 The LED output is stabilized before the tube is gated on to ensure that the rise-time measurement is representative of the detector configuration

6. Test Results

Measured values for PMT signal rise time, hold-off ratio, gate voltage, LED voltage input level, and respective applied cathode voltage are reported in table 3

6.1. Bialkaline Photocathode Tubes

Photomultipliers with bialkaline photocathodes previously used in DIAL applications have characteristically produced a ramped anode signal This ramping effect or change in output signal gain can be observed during a single 40-μs-wide gate pulse or each sequential gate pulse of a sequence control cycle at 1, 5, or 10 Hz Figure 11 illustrates this characteristic produced by an RCA C7268 tube with standard focus-grid base Although gain change in PMT's can sometimes be associated with tube current, the signal gain of the RCA C7268 is predominantly affected during the focus-grid-gating sequence Evidence of this effect from gating the grid is shown in the anode-signal behavior when the leading edge of a wide LED pulse ($>$ 1 ms) is moved from the beginning of a focus-gate sequence into the sequence (See figs 12(a) and (b)) The respective anode responses shown in figure 12(c) indicate that gain change over the focus-gate sequence is affected by grid gating and not LED signal changes or PMT current effects Further tests were conducted in an effort to determine the cause of the output signal variation in gated bialkaline tubes These tests included heating a bialkaline tube to reduce photocathode resistivity and varying LED duty cycles with PMT gating Gain stability increased with the photocathode temperature but remained the same during tests which varied LED duty cycles with tube gating Although these tests were not conclusive, they did indicate possible correlation of gain stability to photocathode cesium migration (ref 6) and/or charge redistribution on the photocathode due to rapid changes in the focus-grid potential

Other bialkaline cathode tubes which exhibit similar gain change characteristics include the RCA 4501/V4 and the QUANTACON PMT's, namely the RCA 8850 and C31000M QUANTACON PMT's employ an extremely high-gain gallium phosphide (GaP) first dynode This type dynode provides an increase of up to an order of magnitude in secondary-emission ratio over conventional dynode materials QUANTACON tubes are also designed to operate with a high potential ($\approx$ 600 to 1000 V) between the cathode and first dynode Due to a gating-voltage limitation of approximately 300 V, these tubes are operated at a lower cathode to dynode 1 potential No abnormal tube behavior was noted from this voltage limitation

The Hamamatsu R1332 PMT with a GaP first dynode exhibited considerable improvement in gain stability when used with the same bases as other bialkaline tubes Due to the increased gain stability, signal averaging using the DEC PDP-11/10 minicomputer and data processing software was required to detect the change in gain of the R1332 over an individual focus gate and the focus-gate sequence A 2- to 3-percent change in the anode output signal was measured from the first through the tenth focus gate over a 1000-shot average Less than a 2-percent change in the signal was measured over a single 40-μs-wide focus gate, compared with approximately 15 percent for the RCA C7268 tube It must be noted that the R1332 is a QUANTACON type PMT and has been tested in voltage-divider networks with less than optimum voltage distributions

Dynode-gated bases L-100-G and A1 demonstrated better gain stability when configured with bialkaline tubes as compared with the focus-grid-gated bases but only over a narrow range of operating parameters Any changes in gate voltage, supply voltage, and light input that vary tube current also affect the gain characteristics of the PMT The gate voltage is varied to demonstrate gain change as influenced by gate voltage while the LED output is held constant as shown in figure 13 Figure 14 demonstrates gain change as a function of light input and tube current These characteristics limit the operation of the dynode-gated bases tested to a specific gate voltage, supply voltage, and tube current Lack of flexibility in tube operation parameters makes the dynode-gated bases poor candidates for DIAL applications

Hold-off ratios for the bialkaline tubes tested in focus-grid bases ranged from a ratio of 2×10^3 1 to better than 10^4 1 Hold-off ratios for the dynode-gated bases were less in all cases and ranged from 2×10^2 1 for the RCA 8850 tube to 8×10^2 1 for the RCA C31000M tube

The Hamamatsu R1332 PMT with the focus-grid base produced a rise time of 0 5 μs, whereas the rise times measured for the RCA C31000M and 4501/V4 tubes in the focus-grid bases were between 0 8 and 1 6 μs However, the characteristic ramp on the RCA C7268 anode signal prevented an accurate rise-time measurement The rise times exhibited by all bialkaline tubes with the dynode-gated base were between 0 8 and 1 2 μs

6.2. Multialkaline Photocathode Tubes

The EMI 9817QB, RCA 7265, and RCA 8852 PMT's possess a multialkaline (NaKCsSb) photocathode which has been predominantly used in DIAL aerosol mapping applications The EMI 9817QB tube, however, with the quartz window and S-20 cathode coating has a spectral response that extends into the UV energy region with a quantum efficiency peak around 290 nm These tubes did not exhibit the high degree of gain change previously shown to be

characteristic of bialkaline tubes in the gated-focus-grid configurations A comparison of multialkaline PMT output signals (figs 15, 16, and 17) with a typical bialkaline tube signal (fig 11(c)) illustrates the significant improvement in gain stability

The EMI 9817QB tube was tested in a dedicated 12-stage focus-grid-gated base (base 6) similar to the 14-stage bases used with the RCA tubes The change in signal gain of this detector configuration stayed within 2 to 3 percent over a complete gating sequence (fig 15(a)) and under 1 percent during a single 40-μs gate pulse (fig 15(b)) The tube also exhibited the fastest rise time at 0 4 μs and a hold-off ratio of better than 10^4 1 These performance characteristics combined with the ability of the 9817QB to detect in the UV energy region make it an excellent replacement tube for the bialkaline tubes and a candidate for UV applications

Evaluation tests of the RCA 7265, as for the RCA C7268, were restricted to focus-grid-gated bases 2 and 4, because of PMT and base dimensions Gain stability and rise-time results were slightly better for the RCA 7265 and 8852 PMT's with base 4 than in similar tests performed with base 2 Rise times in both tubes increased from approximately 0 5 μs when configured with base 4 to between 1 0 and 2 0 μs with base 2 Gain stability also varied between bases The anode output of an RCA 7265 PMT with bases 2 and 4, with identical test parameters, is shown in figures 16 and 17 The increased gain stability shown with base 4 can largely be explained by the larger capacitors connected in parallel in the later dynode stages The larger capacitors provide base 4 with a higher current capacity in the latter stages and better stabilize the voltage distribution between dynodes which, in turn, stabilize the gain for better pulse response Hold-off, however, is not affected by the difference in capacitor values and remains essentially the same for both focus-grid bases Both the RCA 7265 and 8852 tubes exhibited hold-off ratios of better than 4×10^3 1

Performance of the RCA 8852 PMT in the dynode-gated bases, A1 and L-100-G, closely followed the same characteristic trends displayed by the bialkaline tubes but with a hold-off switching ratio between 5×10^2 1 and 6×10^2 1

7. Concluding Remarks

A detector test system has been developed and assembled for evaluating photodetector packages used in support of the DIAL lidar system at the Langley Research Center A study using this facility to simulate lidar conditions was conducted to determine selected photomultiplier tube (PMT) signal characteristics Detector packages tested consisted of PMT's with multialkaline and bialkaline photocathodes and gatable voltage-divider networks using the focus-grid or dynodes as the gating element The characteristics investigated to determine optimal detector performance were hold-off or switching ratios, signal rise time, and gain stability A summary of results and parameters for each detector package examined in this study has been tabulated

The dynode-gated bases failed to show the flexibility in operating parameters required for lidar application Output signal gain of all the dynode-gated detectors tested was affected by any change in gate voltage and output signal levels Switching ratios were also found to be poor ($< 8 \times 10^2$ 1) when these bases were used with the bialkaline tubes Rise time, however, was not found to be a major factor in detector selection since all base and PMT combinations produced rise times of approximately 1 μs

The voltage-divider networks using the focus grid for tube gating produced acceptable lidar signal characteristics with multialkaline tubes These detector packages illustrated performance characteristics sufficient for lidar aerosol applications in the visible portion of the spectrum In addition, the performance of the EMI 9817QB tube makes it a viable multialkaline PMT for lidar applications in the ultraviolet (UV) wavelength region With the exception of the Hamamatsu R1332, the bialkaline tubes with the focus-grid bases showed a 5- to 15-percent change in signal level over the constant portion of a pulsed light input signal The Hamamatsu R1332, however, showed less than a 2-percent change in signal over the same portion of input signal A borosilicate glass window restricts the R1332 from presently being used for UV lidar applications This restriction can be corrected with a factory-installed quartz window

This study has been instrumental in the selection of improved photo detector packages for the DIAL system The change in gain noticed in DIAL detectors has been investigated and minimized by the use of select detectors and bases This optimization increases the accuracy and confidence levels of lidar data and interpretation of results Detector configurations using the EMI 9817QB and Hamamatsu R1332 tubes exhibited increased gain stability over previously used bialkaline cathode tubes, therefore, alternative and improved UV DIAL detectors are provided As a result, the EMI 9817QB PMT was selected and has since been used successfully in a detector package for DIAL flight experiments It has been further concluded that the development of viable gatable voltage-divider networks for bialkaline photocathode PMT's is needed and the cause of gain instability should be pursued and determined

Acknowledgments

The author wishes to thank A F Carter of the Langley Research Center for his invaluable contributions and guidance during this investigation and to recognize W J McCabe and N L McRae of Langley for their excellent technical support in the development of the detector test facility Appreciation is also expressed to C F Butler of the Old Dominion University Research Foundation, Norfolk, Virginia, for software development, and to R J Allen of Old Dominion for his expertise in detector associated electronics

NASA Langley Research Center
Hampton, VA 23665-5225
April 30, 1986

References

1 Engstrom, Ralph W *Photomultiplier Handbook* PMT-62, RCA Corp , c 1980 (Supersedes PT-61, Sept 1970)

2 Browell, E V , Carter, A F , Shipley, S T , Allen, R J , Butler, C F , Mayo, M N , Siviter, J H , Jr , and Hall, W M The NASA Multipurpose Airborne DIAL System and Measurements of Ozone and Aerosol Profiles *Appl Opt* , vol 22, no 4, Feb 15, 1983, pp 522–534

3 Butler, Carolyn F , Shipley, Scott T , and Allen, Robert J *Investigation of Potential of Differential Absorption Lidar Techniques for Remote Sensing of Atmospheric Pollutants* Tech Rep GSTR-81-8 (Grant NSG-1477), Old Dominion Univ , July 1981 (Available as NASA CR-164645)

4 Hunt, W H , and Poultney, S K Testing the Linearity of Response of Gated Photomultipliers in Wide Dynamic Range Laser Radar Systems *IEEE Trans Nucl Sci* , vol NS-22, no 1, Feb 1975, pp 116–120

5 Bethke, George W *Development of Range Squared and Off-Gating Modifications for a Lidar System* EPA-650/2-73-040, U S Environmental Protection Agency, 1973 (Available from NTIS as PB 228 715)

6 Cathey, L Fatigue in Photomultipliers *IRE Trans Nucl Sci* , vol NS-5, no 3, Dec 1958, pp 109–114

TABLE 1 SUMMARY OF PMT DATA

[KCsSb bialkaline cathode, NaKCsSb multialkaline cathode]

PMT manufacturer and type	Photo-cathode material	Window material	Recommended voltage distribution[1]	Number of stages	Wavelength of maximum response (±50 nm)	Wavelength range, nm	Maximum voltage (K to P)[1], V	Remarks
RCA 7265	NaKCsSb	Borosilicate glass	W	14	420	300 to 820	3000	
RCA C7268	KCsSb	Fused silica	W	14	420	180 to 660	3000	UV variant of RCA 7265 PMT
RCA C31000M	KCsSb	Fused silica	T	12	400	180 to 660	3000	UV variant of RCA 8850 PMT QUANTACON type (Dy1 GaAsP)
RCA 4501/V4	KCsSb	Fused silica	S	12	400	180 to 660	2500	
RCA 8852	NaKCsSb	Pyrex	T	12	575	260 to 920	2500	Variant of 8850 PMT ERMA III photocathode
RCA 8850	KCsSb	Pyrex	T	12	385	260 to 660	3000	QUANTACON type (Dy1 GaAsP)
Hamamatsu R1332	KCsSb	Borosilicate glass	T	12	420	300 to 650	2700	8850 replacement tube (Dy1 GaAsP)
EMI 9817QB	NaKCsSb	Fused silica	R	12	280 and 420	180 to 800	2800	S-20 photocathode coating with quartz window

[1]See table 2

TABLE 2 VOLTAGE DISTRIBUTIONS

[Adapter, RCA AJ2132, K, cathode, Dy, dynode, and P, anode]

No of stages	Base/distribution code	Voltage distribution K, Dy1, Dy2, Dy3, , P
12	R	2, 1, 1, 1, 1, 1, 1, 1, 1, 1, 1, 2, and 1
	S	4, 1, 1 4, 1, 1, 1, 1, 1, 1, 1, 1, 1, and 1
	T	6, 1, 1 4, 1, 1, 1, 1, 1, 1, 1, 1, 1, and 1
	Base 2 with adapter	3, 1, 1, 1, 1, 1, 1, 1, 1, 1, 1 1, 1 25, and 1 4
	Base 4 with adapter	3, 1, 1, 1, 1, 1, 1, 1, 1, 1 2, 1 5, 2, and 2
	Base L-100-G	6, 1, 1 5, 1, 1, 1, 1, 1, 1, 1 2, 1 5, 1 8, and 2
	Base A1	7, 1, 1 4, 1, 1, 1, 1, 1, 1, 1, 1, and 1
	Base 6	2 4, 1, 1, 1, 1, 1, 1, 1, 1, 1 25, 1 4, 1 75, and 2 5
14	W	2, 1, 1, 1, 1, 1, 1, 1, 1, 1, 1, 1 25, 1 5, 1 75, and 2
	Base 2	3, 1, 1, 1, 1, 1, 1, 1, 1, 1, 1, 1 1, 1 25, and 1 4
	Base 4	3, 1, 1, 1, 1, 1, 1, 1, 1, 1, 1 2, 1 5, 2, and 2

TABLE 3 PMT PERFORMANCE DATA

[Gain stability measurements made during rectangular LED pulses of 40 μs and PMT signals of 200 mV, all detector configurations with L-100-G and A1 bases exhibited gain-stability dependence on gate voltage and tube current]

PMT type	Base	Cathode voltage, V	Gate voltage, V	Anode output, mV	Bleed-through, mV	Hold-off ratio	Rise time, μs
Bialkaline photocathode							
RCA 4501/V4[a]	2	−1800	200	400	< 0 05	$> 10^4$ 1	1 5
	4	−1800	210	400	< 05	$> 10^4$ 1	8
	L-100-G	−1800	185	200	5	4×10^2 1	1 2
RCA C31000M[a]	2	−1800	290	400	0 1	4×10^3 1	1 6
	4	−1800	270	400	1	4×10^3 1	1 2
	A1	−1800	210	400	5	8×10^2 1	1 0
	L-100-G	−1800	190	200	25	8×10^2 1	8
RCA C7268[a]	2	−2200	285	200	< 0 1	$> 2 \times 10^3$ 1	N/A
	4	−2200	290	200	< 1	$> 2 \times 10^3$ 1	N/A
RCA 8850[b]	2	−1800	250	400	0 2	2×10^3 1	2 0
	4	−1800	270	400	2	2×10^3 1	2 0
	A1	−1800	200	400	1 0	4×10^2 1	1 0
	L-100-G	−1800	185	200	1 0	2×10^2 1	1 0
Hamamatsu R1332[c]	2	−1800	260	400	< 0 05	$> 10^4$ 1	1 5
	4	−1800	260	400	< 05	$> 10^4$ 1	5
	A1	−1800	190	200	5	4×10^2 1	1 0
	L-100-G	−1800	200	200	5	4×10^2 1	1 0
Multialkaline photocathode							
RCA 8852[b]	2	−1800	275	400	0 1	4×10^3 1	1 0
	4	−1800	260	400	1	4×10^3 1	5
	A1	−1800	200	400	8	5×10^2 1	2
	L-100-G	−1800	190	150	25	6×10^2 1	
RCA 7265[b]	2	−1800	300	400	0 1	4×10^3 1	1 9
	4	−1800	300	400	1	4×10^3 1	6
EMI 9817QB[d]	6	−1800	220	400	< 0 05	$> 10^4$ 1	0 4

[a] Gain change measured to be $\approx$ 15 percent with bases 2 and 4
[b] Gain change measured to be $\leq$ 5 percent with bases 2 and 4
[c] Gain change measured to be $\leq$ 2 percent with bases 2 and 4
[d] Gain change measured to be $\leq$ 1 percent

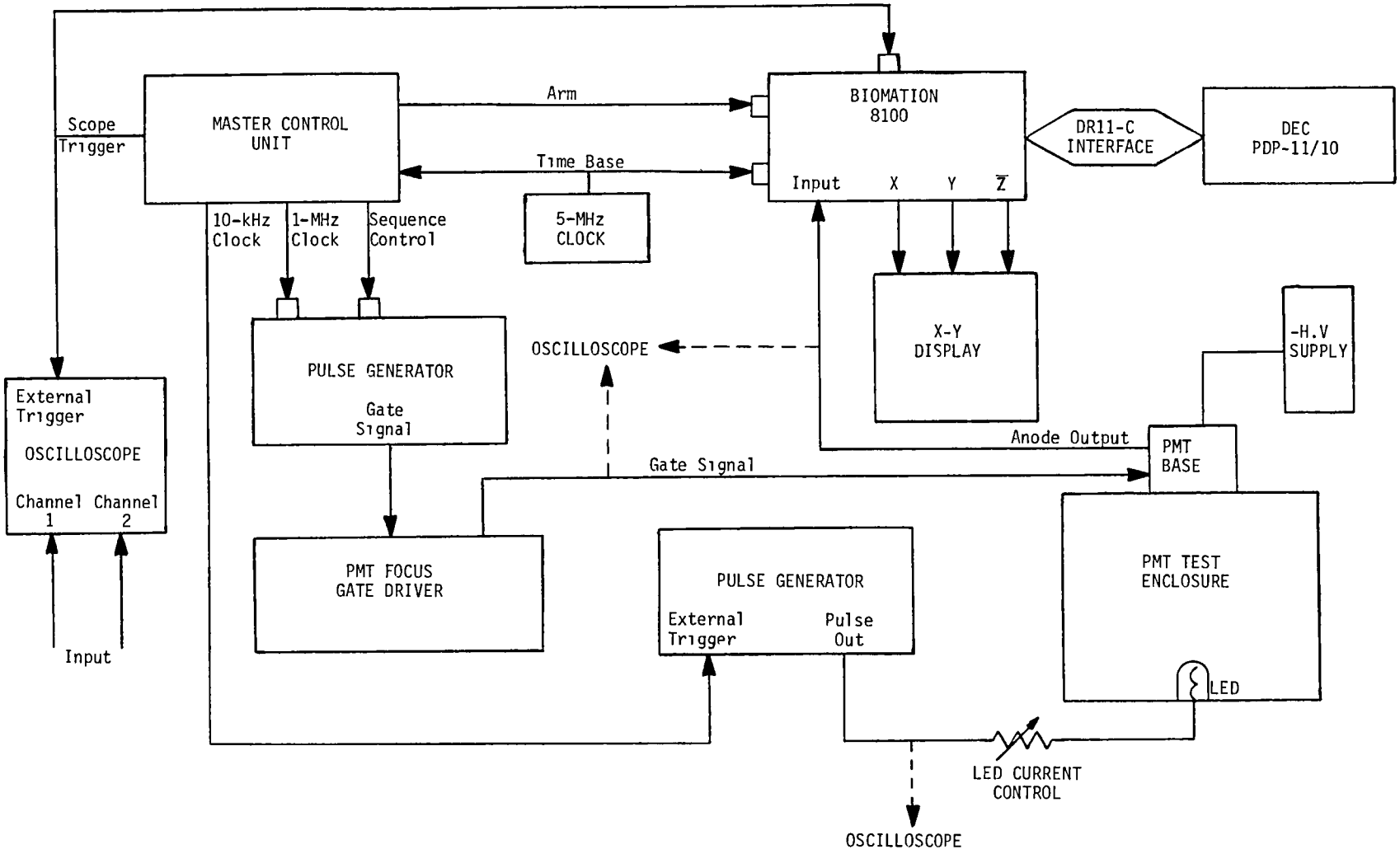

Figure 1 PMT test and data acquisition system

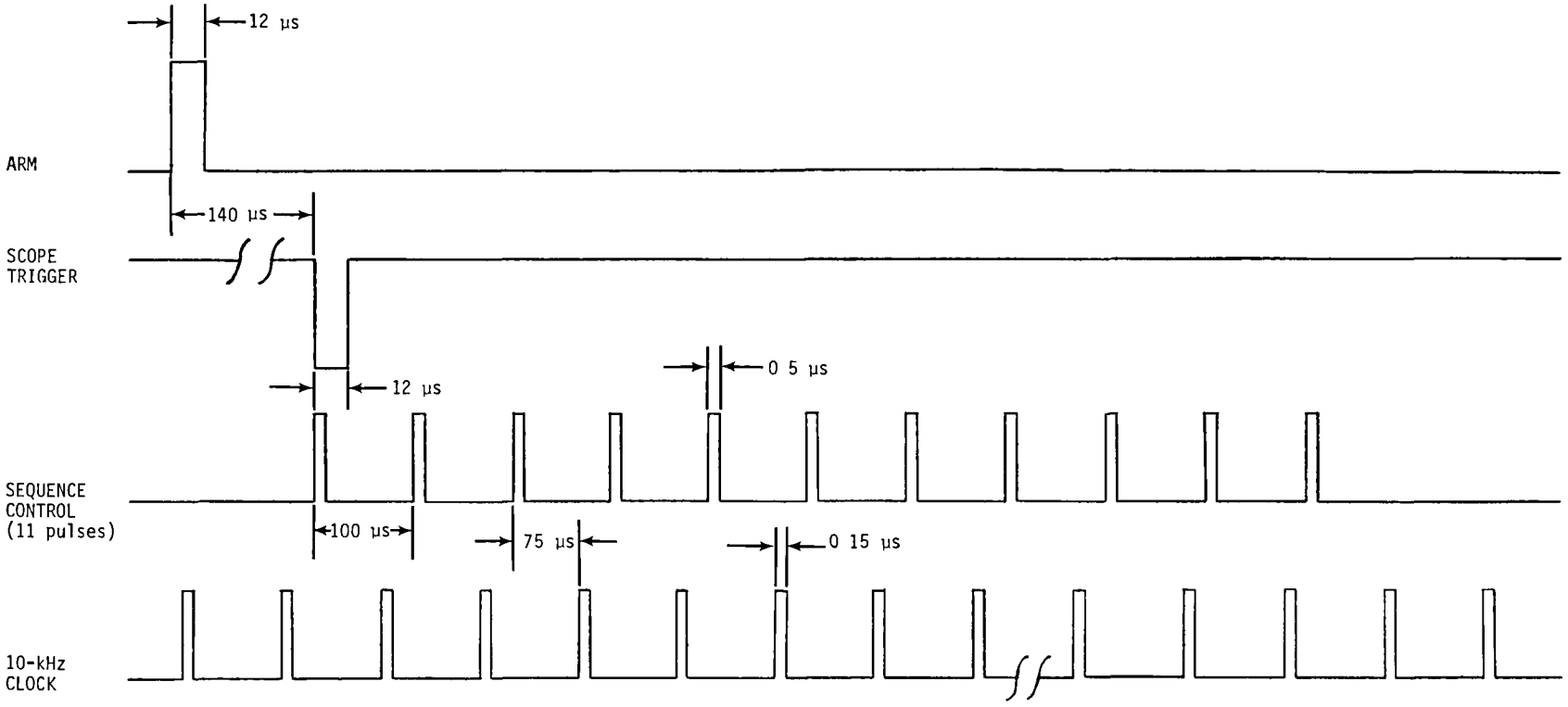

Figure 2 Timing signals from master control unit

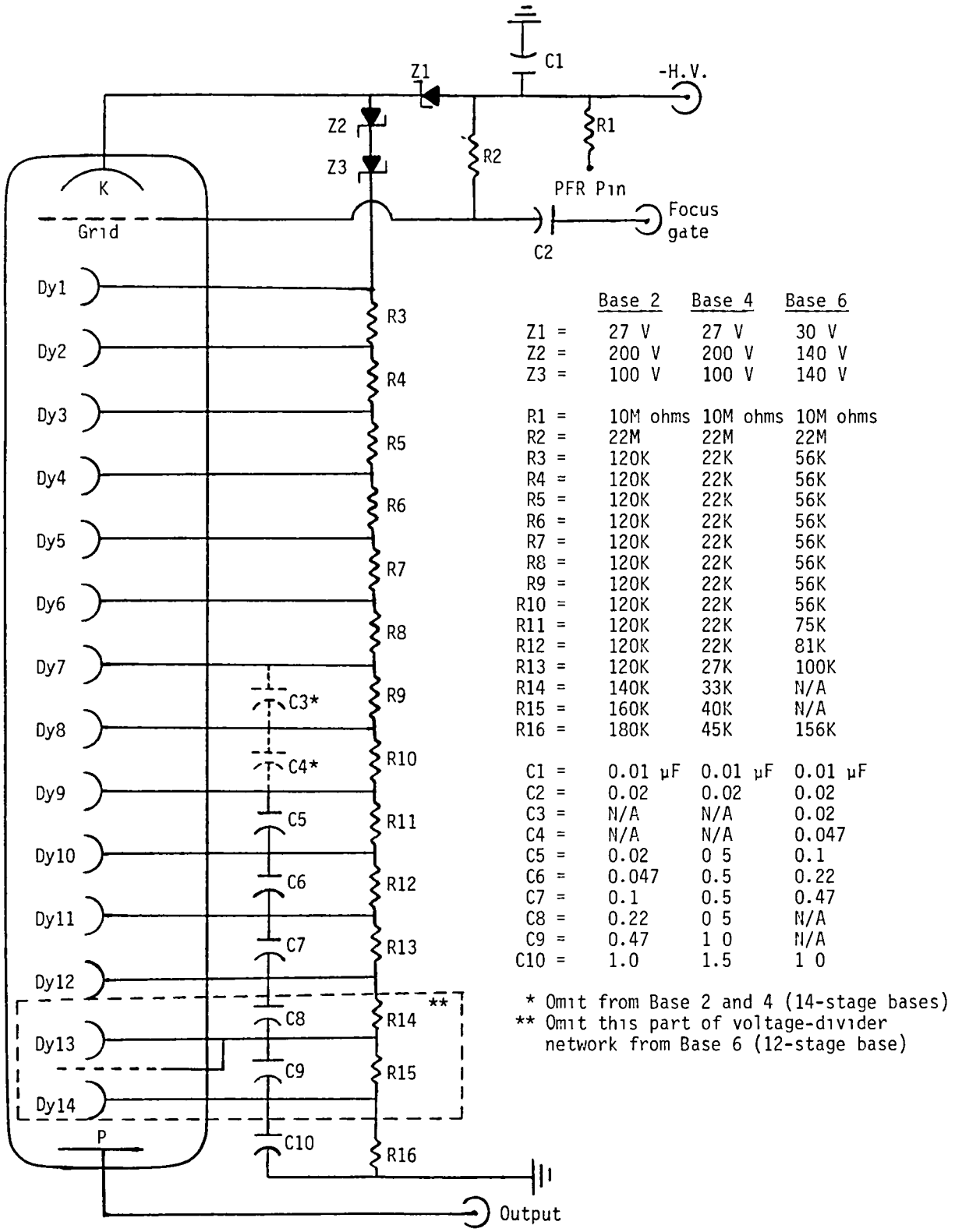

	Base 2	Base 4	Base 6
Z1 =	27 V	27 V	30 V
Z2 =	200 V	200 V	140 V
Z3 =	100 V	100 V	140 V
R1 =	10M ohms	10M ohms	10M ohms
R2 =	22M	22M	22M
R3 =	120K	22K	56K
R4 =	120K	22K	56K
R5 =	120K	22K	56K
R6 =	120K	22K	56K
R7 =	120K	22K	56K
R8 =	120K	22K	56K
R9 =	120K	22K	56K
R10 =	120K	22K	56K
R11 =	120K	22K	75K
R12 =	120K	22K	81K
R13 =	120K	27K	100K
R14 =	140K	33K	N/A
R15 =	160K	40K	N/A
R16 =	180K	45K	156K
C1 =	0.01 μF	0.01 μF	0.01 μF
C2 =	0.02	0.02	0.02
C3 =	N/A	N/A	0.02
C4 =	N/A	N/A	0.047
C5 =	0.02	0 5	0.1
C6 =	0.047	0.5	0.22
C7 =	0.1	0.5	0.47
C8 =	0.22	0 5	N/A
C9 =	0.47	1 0	N/A
C10 =	1.0	1.5	1 0

* Omit from Base 2 and 4 (14-stage bases)
** Omit this part of voltage-divider network from Base 6 (12-stage base)

Figure 3 Circuit diagram of bases 2, 4, and 6 with PMT

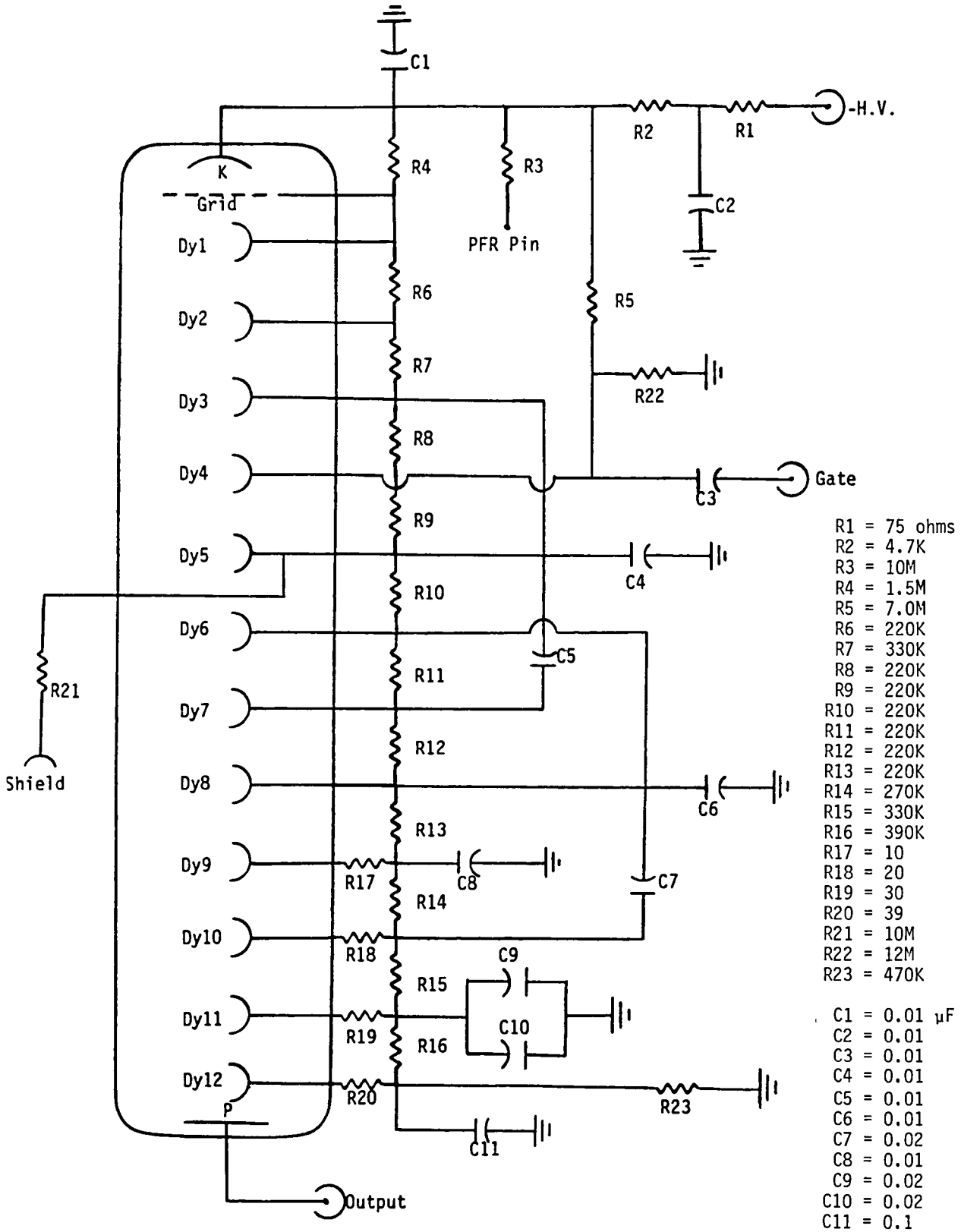

Figure 4 Circuit diagram of base L-100-G with PMT

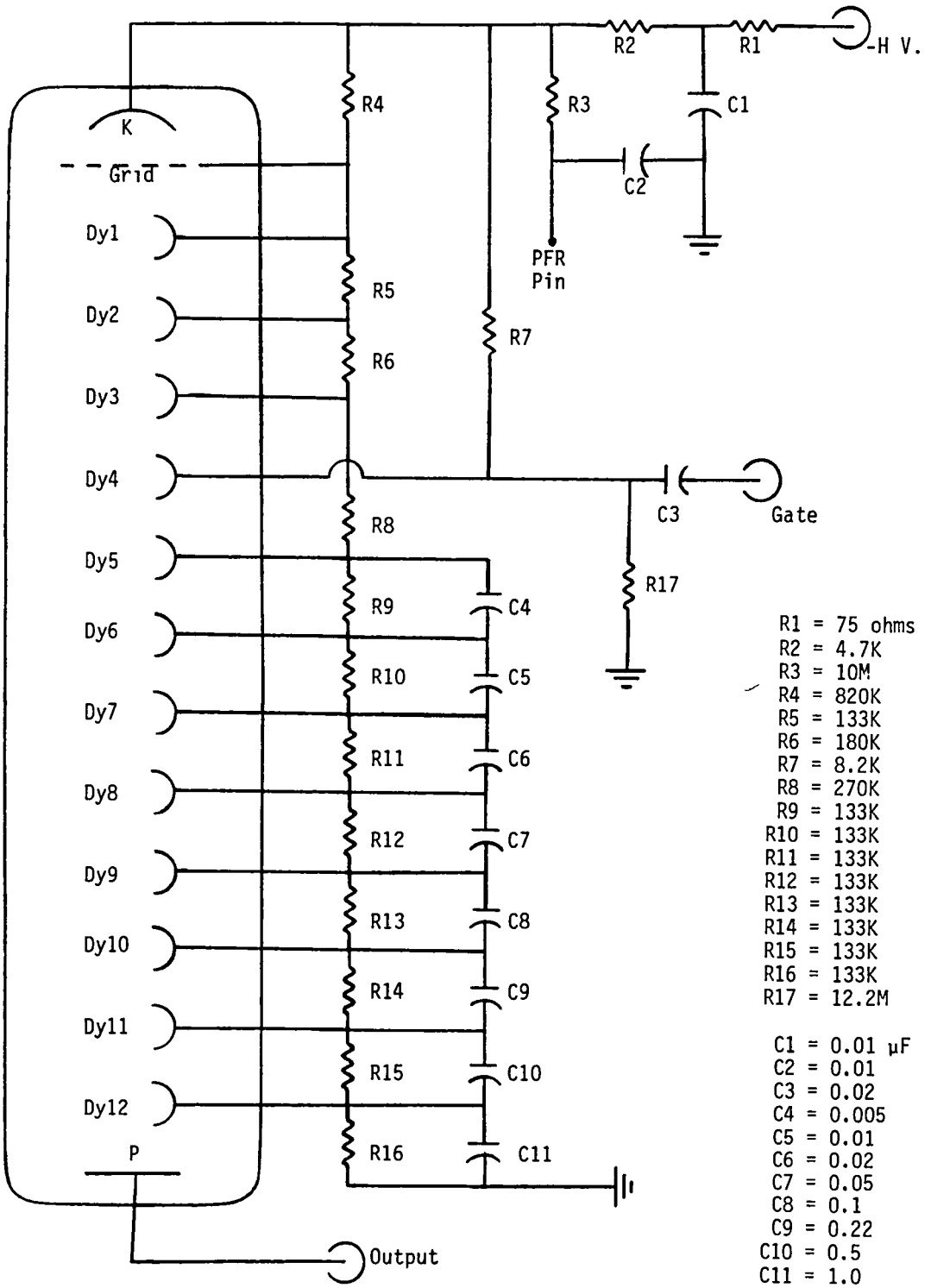

Figure 5 Circuit diagram of base A1 with PMT

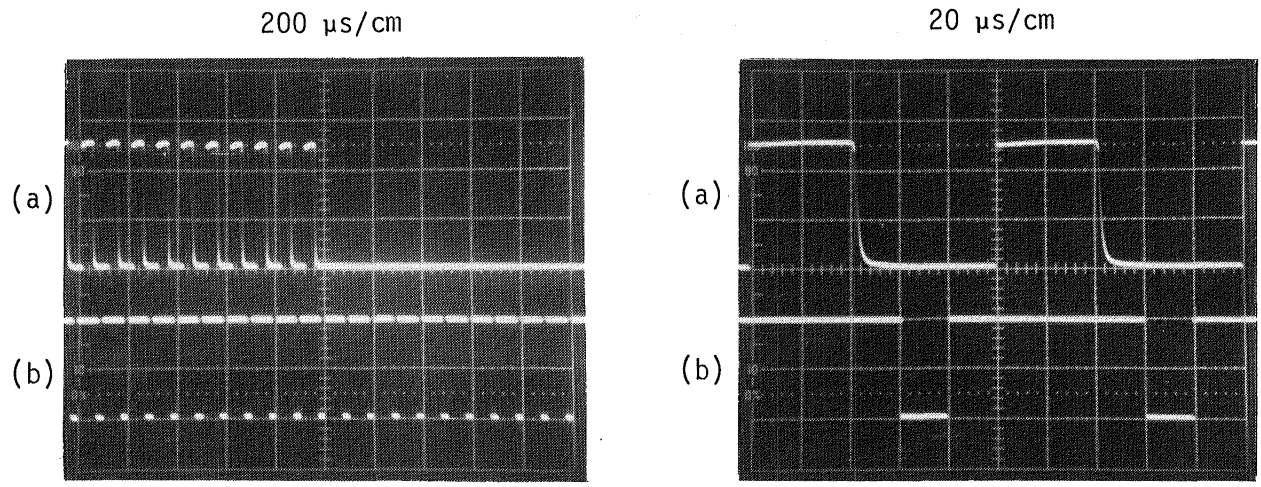

(a) Gate pulses with 100-μs separation intervals at 10-Hz repetition rate.

(b) Continuous LED pulses with 100-μs intervals.

Figure 6. Timing sequences for gate and LED signals.

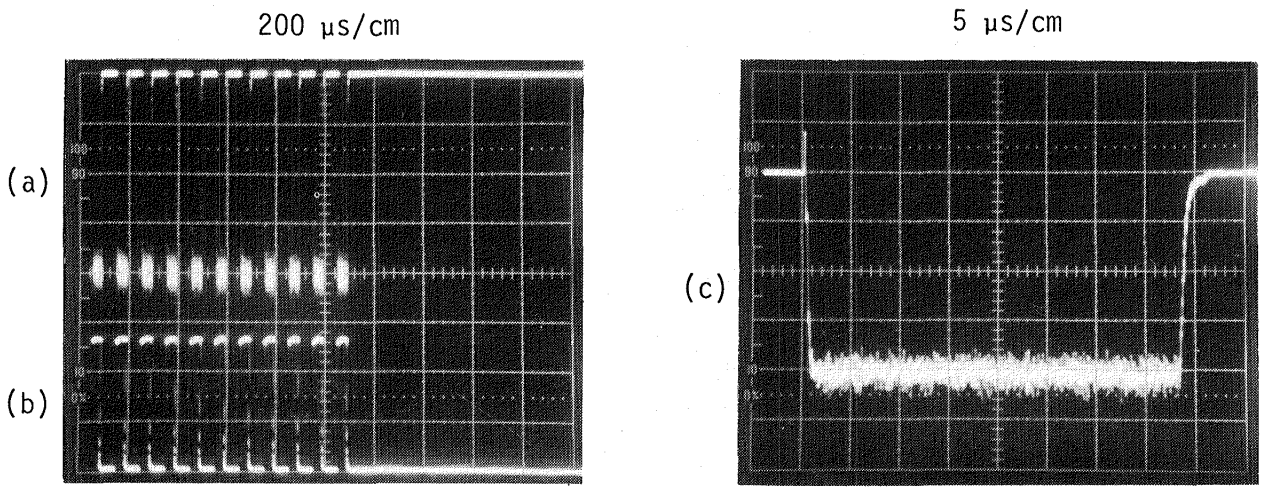

(a) Anode signal; 50 mV/cm.

(b) Focus-gate signal; 100 V/cm.

(c) Anode signal during single gate pulse; 50 mV/cm.

Figure 7. Anode signal from Hamamatsu R1332 PMT (bialkali) with base 4.

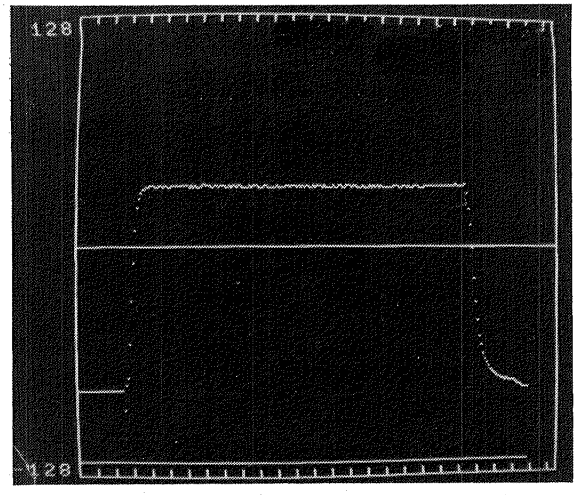

Figure 8. Digitized anode signal. Sample interval, 0.1 μs; range, 0.2 V; 200-shot average.

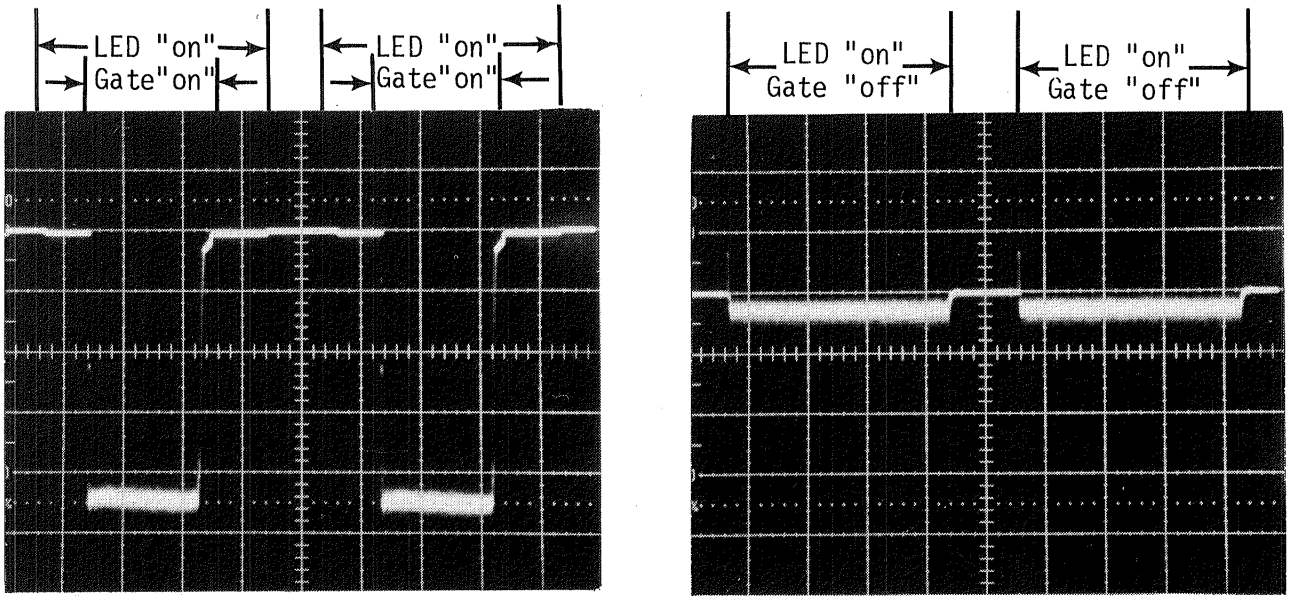

(a) 400-mV anode signal from two 40-μs gate signals during 80-μs LED pulses; 100 mV/cm.

(b) Anode signal (bleedthrough) from 80-μs LED pulses with gate off; 2 mV/cm.

Figure 9. Anode signal for hold-off measurements.

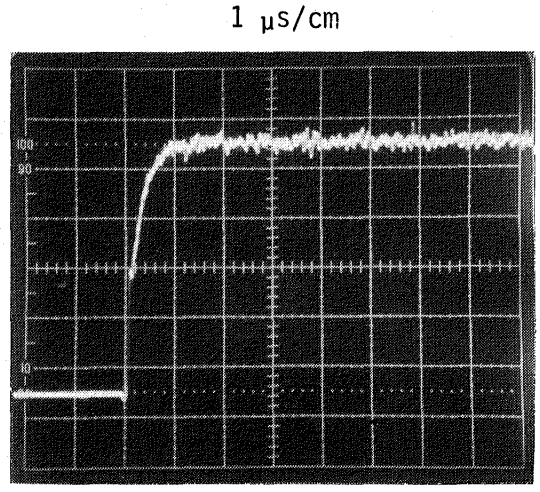

Figure 10. Leading edge of inverted anode signal used for rise-time measurements. 50 mV/cm.

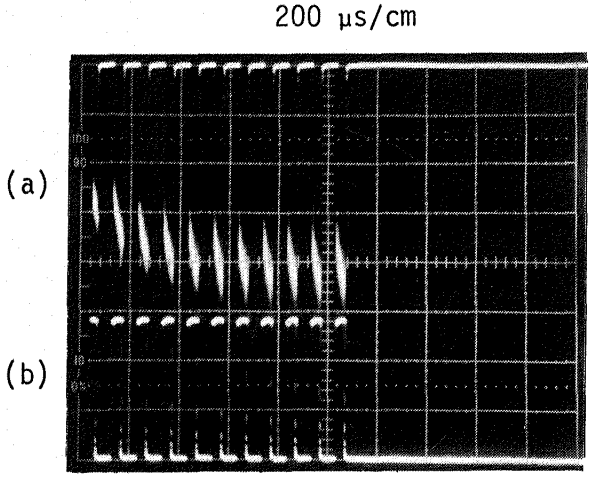

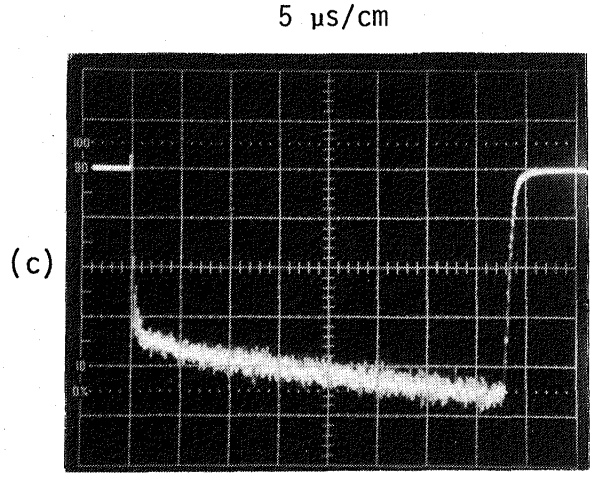

(a) Anode output; 50 mV/cm.

(b) Focus-gate signal; 100 V/cm.

(c) Anode output during fifth focus gate.

Figure 11. Output signal from RCA C7268 PMT (bialkali) with base 4.

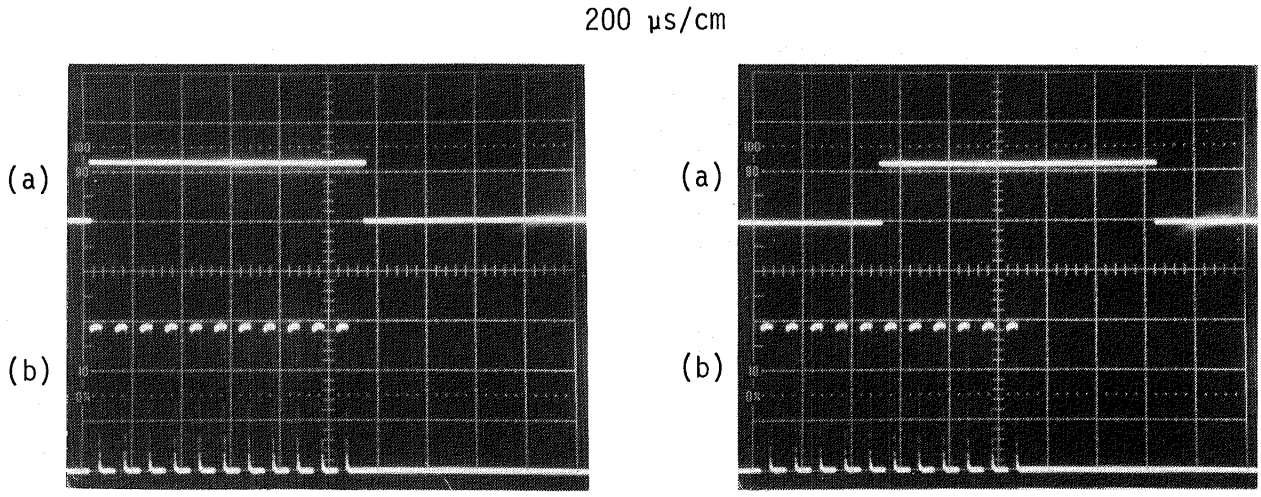

(a) LED pulse; 2 V/cm.

(b) Focus-gate signal; 100 V/cm.

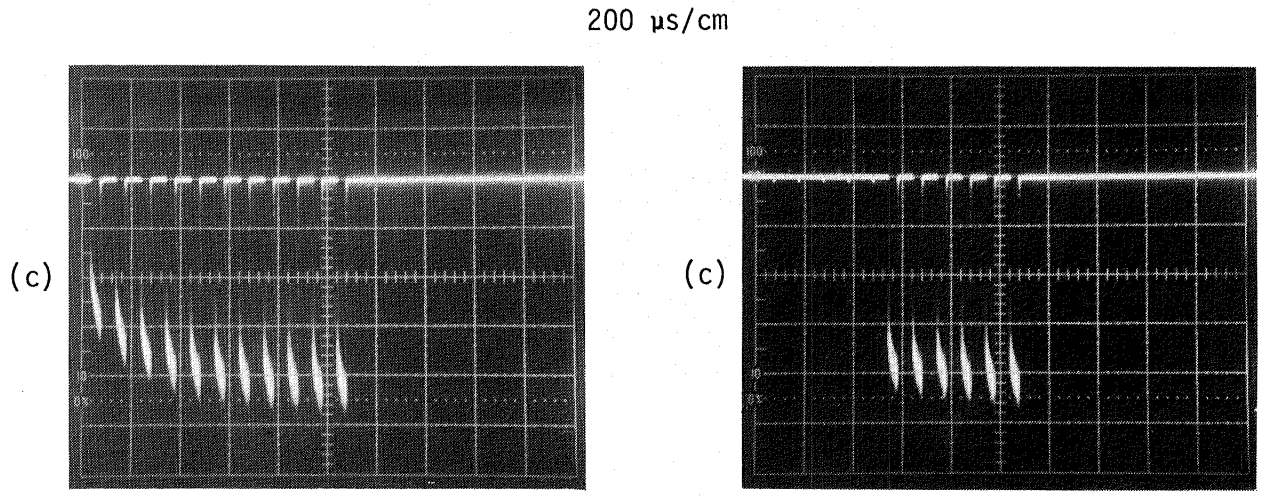

(c) Anode signal; 50 mV/cm.

Figure 12. Gated-focus grid effect on anode signal from RCA C7268 PMT (bialkali) with base 2.

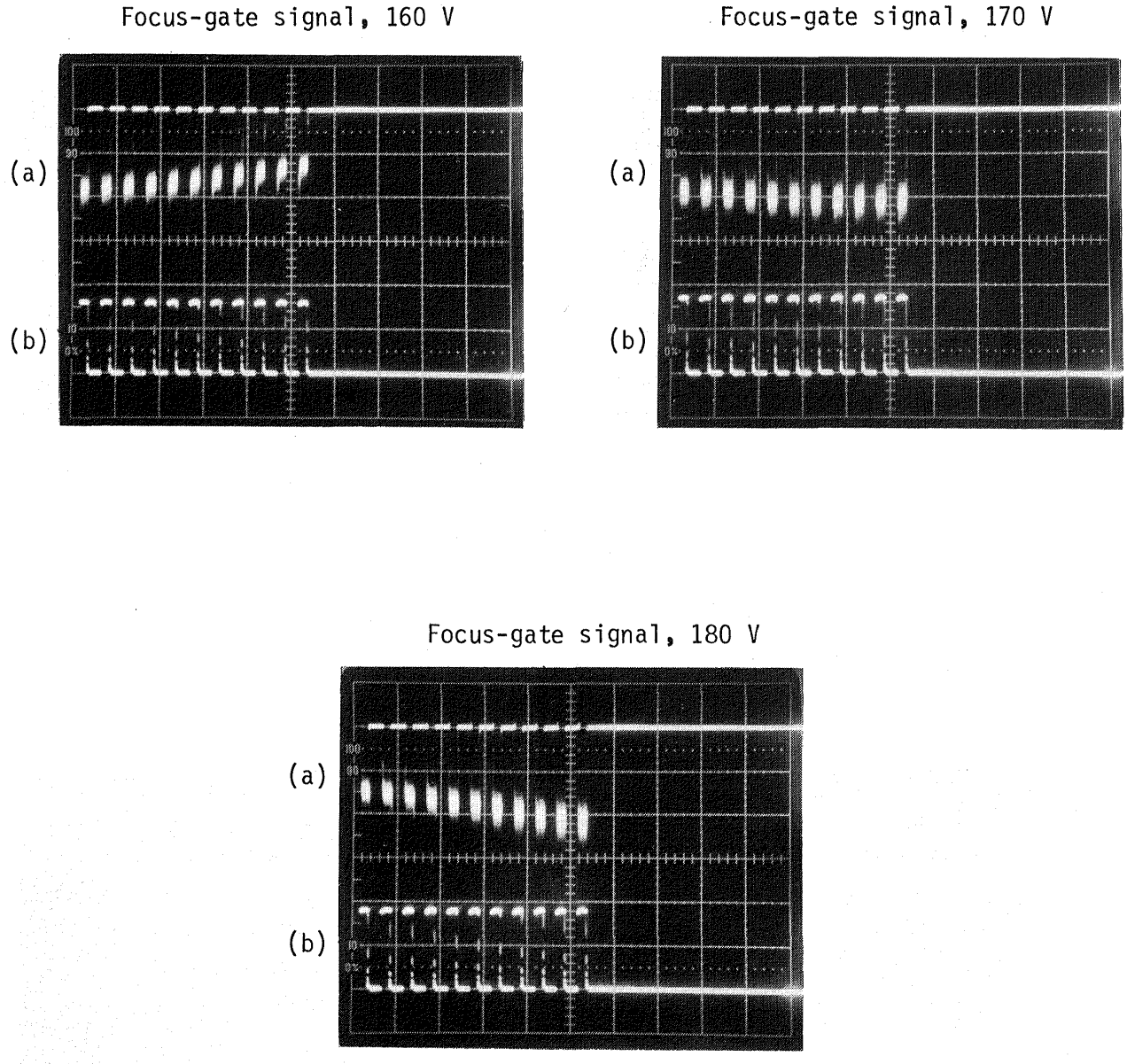

(a) Anode signals; 50 mV/cm.

(b) Focus-gate signal; 100 V/cm.

Figure 13. Dynode-gating base characteristics from RCA C31000M PMT (bialkali) with base L-100-G for varied focus-gate signals and constant LED pulse. 200 μs/cm.

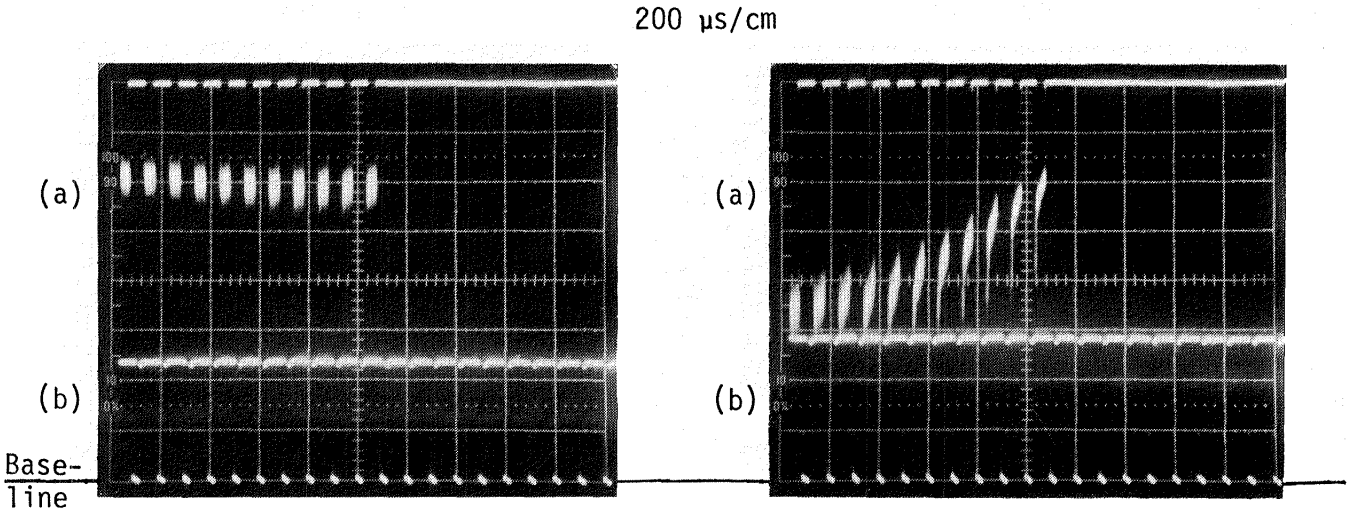

(a) Anode signals; 50 mV/cm.

(b) LED pulse; 1 mV/cm.

Figure 14. Dynode-gating base characteristics from RCA C31000M PMT (bialkali) with base L-100-G for constant focus-gate signal level and varied LED pulse. 200 μs/cm.

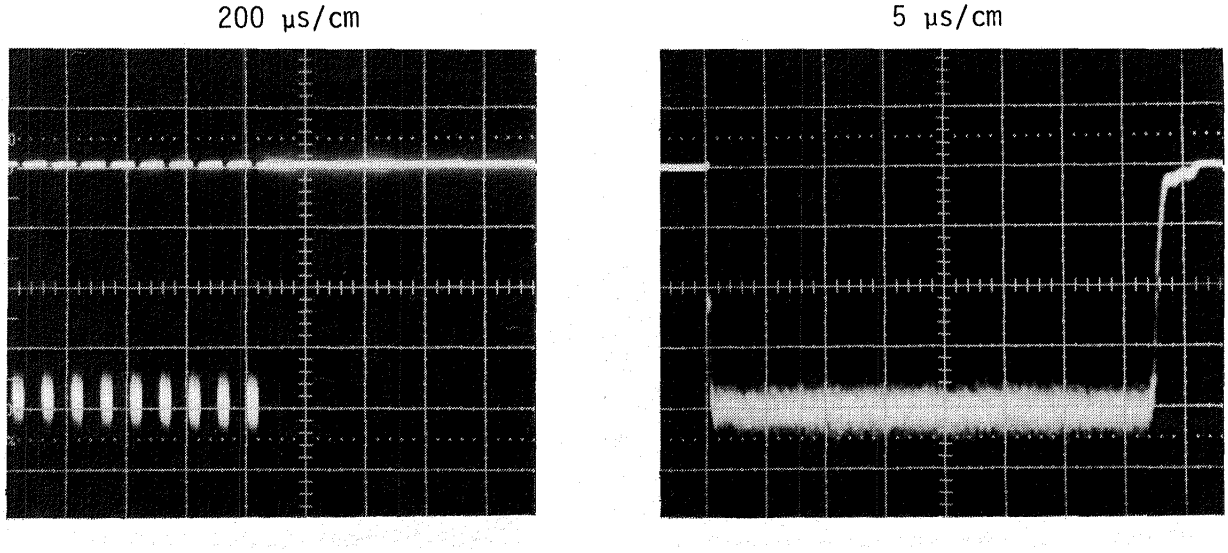

(a) Anode signal during gating sequence.

(b) Anode signal during single gate pulse.

Figure 15. Anode signal from EMI 9817QB (multialkali) with base 6. 100 mV/cm.

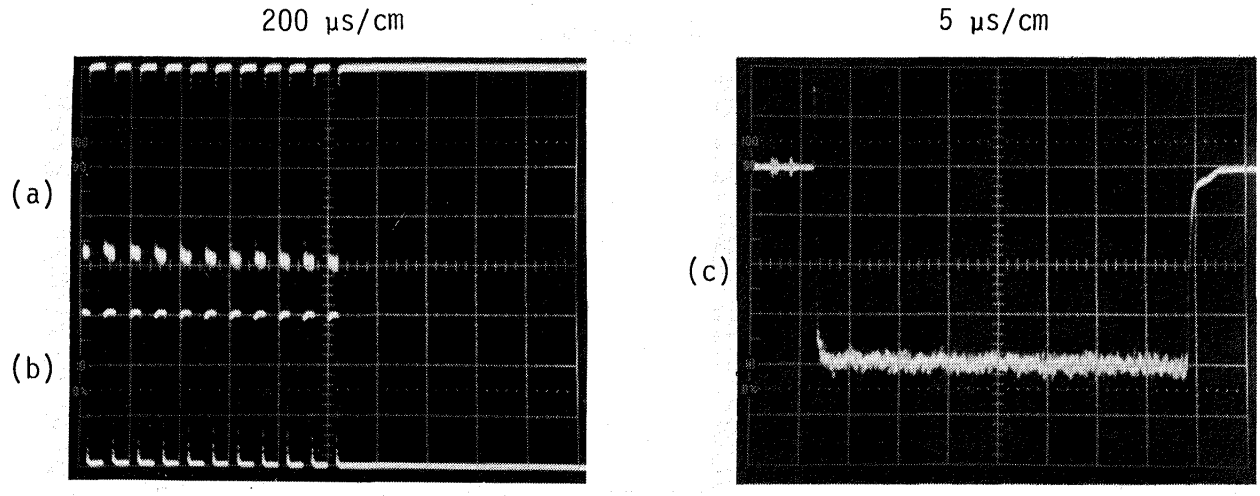

(a) Anode signal; 50 mV/cm.

(b) Focus-gate signal; 100 V/cm.

(c) Anode signal during fifth focus gate; 50 mV/cm.

Figure 16. Anode signal from RCA 7265 PMT (multialkali) with base 4.

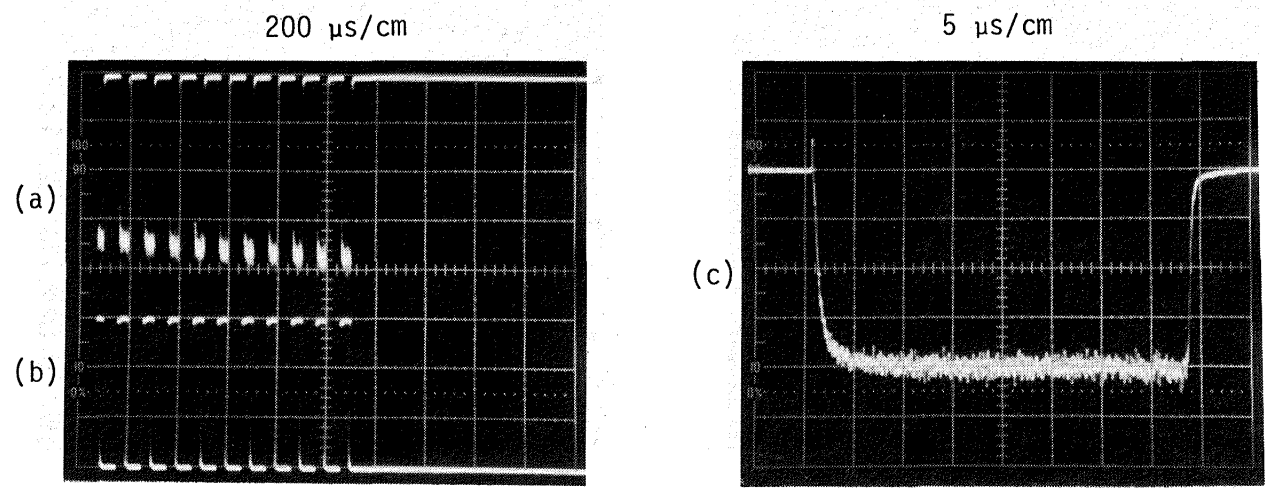

(a) Anode signal; 50 mV/cm.

(b) Focus-gate signal; 100 V/cm.

(c) Anode signal during fifth focus gate pulse; 50 mV/cm.

Figure 17. Anode signal from RCA 7265 PMT (multialkali) with base 2.

End of Document